Hydrol. Earth Syst. Sci. Discuss., https://doi.org/10.5194/hess-2018-581
Manuscript under review for journal Hydrol. Earth Syst. Sci.
Discussion started: 11 December 2018

Hydrology and Earth System Sciences
Discussions
Open Access

A Unique Vadose Zone Model for Shallow Aquifers: the Hetao Irrigation District, China

Zhongyi Liu[1,2], Xingwang Wang[1], Zailin Huo[1*], Tammo Siert Steenhuis[2*]

[1]Center for Agricultural Water Research in China, China Agricultural University, Beijing, 100083, PR China

[2]Department of Biological and Environmental Engineering, Cornell University, Ithaca, NY, USA.

Correspondence to: Zailin Huo (huozl@cau.edu.cn)
Tammo S. Steenhuis (tammo@cornell.edu)

Hydrol. Earth Syst. Sci. Discuss., https://doi.org/10.5194/hess-2018-581
Manuscript under review for journal Hydrol. Earth Syst. Sci.
Discussion started: 11 December 2018

Hydrology and Earth System Sciences
Open Access
Discussions

Abstract

Rapid population growth is increasing pressure on the world water resources. Agriculture will require crops to be grown with less water. This is especially the case for the closed Yellow River basin necessitating a better understanding of the fate of irrigation water in the soil. In this manuscript, we report on a field experiment and develop a physical based model for the shallow groundwater in the Hetao irrigation district in Inner Mongolia, in the arid middle reaches of the Yellow River. Unlike other approaches, this model recognizes that field capacity is reached when the matric potential is equal to the height above the groundwater table and not by a limiting soil conductivity. The field experiment was carried out in 2016 and 2017. Daily moisture contents at 5 depths in the top 90 cm and groundwater table depths were measured in two fields with a corn crop. The data collected were used for model calibration and validation. The calibration and validation results show that the model-simulated soil moisture and groundwater depth fitted well. The model can be used in areas with shallow groundwater to optimize irrigation water use and minimize tailwater losses.

Key words: Hydrological model, Shallow aquifer, Equilibrium state, Soil characteristic curve

1 Introduction

With global climate change and increasing human population, water scarcity in many parts of the world cannot be ignored anymore (Guo and Shen, 2016) and has caused widespread concern among public governmental officials and scientists (Alcamo et al., 2007; Guo and Shen, 2016; Oki and Kanae, 2006). Years of rapid population growth have diminished the world water resources and the global per capita availability of fresh water will be 5100 m^3 by the year 2025, which according to Gardner-Outlaw and Engelman (Gardner-Outlaw and Engelman, 1997), indicates water scarcity and consequently insufficient water for economic development.

In China, which has 22% of the world population and only 7% of the fresh water resources, the amount of water available per capita is only 1700 m^3a^{-1}, when averaged over the whole country (Hinrichsen, 2002). The water shortage in the Yellow River basin is especially severe. The Yellow River produces 33% of the total agricultural production in China, mainly with irrigation from surface and groundwater to overcome the limited rainfall. This irrigation has directly changed the hydrology of the basin. Fifty years ago, the semi-arid North China Plain had springs, shallow groundwater and rivers feeding the Yellow River. Currently, the rivers and springs have dried up and in the last 20 years, groundwater has continuously decreased at rates above 1 m per year (Yang et al., 2015a). At the same time, in the arid Inner Mongolia, along the Yellow River, the once deep groundwater is now within 3 m of the soil surface in the large irrigation projects such as the Hetao irrigation district because of downward percolation of the excess irrigation water that has been applied.

Crop irrigation in the Yellow River basin accounts for 96% of the total water use (Li et al., 2004). Due to increased demands for irrigation, annually the river has stopped flowing downstream for an average of 70 days for the last 10 years (Hinrichsen, 2002). Consequently, during this time, the basin is "closed" and water used in one part cannot be used elsewhere in the basin. Thus, saving water upstream in Inner Mongolia means that more water is available downstream (Gao et al., 2015). Efficient water use can be achieved by field trials measuring the fluxes. This is time consuming, expensive and only a limited set of water management practices can be investigated. Therefore, models have been deployed that can test many management practices, but often are not accurate because they have not been tested under local field conditions. A combination of field experiments, together with physical based models, have the benefits of both approaches with few of the negative effects.

Soil moisture plays a critical role in the growth of crops/vegetation (Rodriguez-Iturbe, 2000), partitioning of rainfall into runoff and infiltration (Merz and Plate, 1997), groundwater recharge and upward movement of water to the rootzone in areas where the groundwater is shallow (Gleeson et al., 2016; Jasechko and Taylor, 2015; Venkatesh et al., 2011).

Simulations of soil moisture content can be roughly grouped into two groups: models that are based on full Darcy's law and those that simplify and regionalize Darcy's law. Both groups use the conservation of mass principles. The full Darcy's law application numerically solves a set of differential equations with a relatively small time-step and areal resolution. These models need, therefore, detailed landscape and soil physical properties and are time consuming to run (Flint et al., 2002). Examples of these models are SHE (Système Hydrologique Européen, Abbott et al., 1986), HYDRUS (Du et al., 2018; Karimov et al., 2018; Wang et al., 2018), SWAP (Soil, Water, Atmosphere and Plant, Su et al., 2005; Wang et al., 2016), and MODFLOW (Mcdonald and Harbaugh, 2003). Simplified and regionalized applications are based on self-organization of the hydrological processes in the landscape. They allow for averaging of the hydrological processes for relatively large landscape units. The main advantages of these models are that generally available data can be used and they can be applied in similar landscapes without the need to collect additional data (Hoang et al., 2017). The disadvantage is that each landscape type has a different set of regionalized landscape parameters. Examples of models using the regionalized Darcy's law are TOPMODEL (Beven and Kirkby, 1979) and SWAT (Soil & Water Assessment Tool) (Neitsch et al., 2000).

In the Yellow River basin, various models were developed to simulate the soil water moisture content, groundwater depth and water fluxes. Finite element or finite difference models that use both Darcy's law and conservation of mass are the Hydrus-1D model (Ren et al., 2016) and Finite Difference Model application (Moiwo et al., 2010). These types of models are valid for any groundwater depth. Simplified and regionalized models are either valid for deep (>3.3m) or shallow groundwater (<3.3m) areas. Models used in the North China Plain with groundwater over 30 m deep were developed by the following researchers: Wang et al. (2001); Kendy et al. (2003); Chen et al. (2010); Ma et al. (2013); Yang et al. (Chen et al., 2010; Kendy et al., 2003; Ma et al., 2013; Wang et al., 2001; Yang et al., 2015a; Yang et al., 2017; Yang et al., 2015b). Usually a unit hydraulic gradient is assumed, and water stops moving when the soil reaches field capacity at 3.3 m (33 kPa) when the hydraulic conductivity becomes limiting.

These models are not valid for irrigation projects along the Yellow River with shallow groundwater because water moves upward from the groundwater to the root zone under a matric potential gradient opposite the gravity potential. Two regionalized models developed for shallow groundwater in the Yellow River basin are by Xue et al. (2018) and Gao et al. (2017). The two models do not consider the dynamics of groundwater depth and matric potential. By including these dynamics, more realistic predictions of moisture contents and upward flow can be obtained and would give better results when extended outside the area where they are developed (Wang and Smith, 2004).

For areas with shallow groundwater, evaporation sets up hydraulic gradient that causes the upward capillary water movement to sustain the evapotranspiration demands and crop water use (Kahlown et al., 2005; Liu et al., 2016; Luo and Sophocleous, 2010; Yeh and Famiglietti, 2009). Water stops moving when the hydraulic potential gradient is zero and thus the matric potential is equal to the height above the water table (in depth units). The moisture content at field capacity (which we call equilibrium moisture content in this manuscript) is thus a function of the groundwater depth and can be found with aid of the soil characteristic curve.

The objective of this study is to develop a novel physical-based model using information of soil characteristic curve and validating this approach using experimental data collected in a field with shallow groundwater. The experimental field is located in the Hetao Irrigation District (HID), Inner Mongolia, China, where on two maize fields, moisture content and the groundwater table depth were measured over a two-year period. The model can be used once validated for saving irrigation water by fine tuning the application amounts.

2 Materials and Methods

2.1 Study Area

The Hetao Irrigation District (HID) is the third largest irrigation district of China. It covers an area of 1.12×10^6 ha of which half is irrigated (Xu et al., 2015). About 5 billion m^3 water are diverted from the Yellow River each year (Xu et al., 2010). The primary irrigation method used is surface flood irrigation (Sun et al., 2013). The groundwater table is very shallow ranging between 0.5 m to 3 m. The overall hydraulic gradient is 0.1-0.25 ‰ (Ren et al., 2018). Soil salinization is serious and the main chemical composition of groundwater salinity mainly consists of NaCl, KCl, $CaSO_4$.The Hetao District has a typical arid continental climate with high evaporation and low rainfall. The average annual precipitation is 180 mm a-1 and the potential evaporation is 2225 mm a^{-1} (Luan et al., 2018). The soil is mainly alluvial deposits with a silty loam texture. It is frozen 5 to 6 months per year from late November to the middle of May. There are about 135-150 frost-free days and an average of 3100-3300 h of sunshine per year (Feng et al., 2005). Maize and wheat are the main food crops and sunflower is the main cash crop.

2.2 Field experiment and data collection

The experiment was carried out in Fenzidi, Bayannur city (41°9′N, 107°39′E) in the Hetao District in 2016 and 2017 (Fig.1). In 2016, the experiment was carried out separately in site A (about 3100 m^2) and site B (about 7000 m^2) (Fig.1). In 2017, Field B was split into Fields C and D and experiments were carried out in these two fields. Field C was about 3400 m^2 and D about 3600 m^2. Experimental fields were planted both years with maize. The sowing date was April 24, 2016 and May 13, 2017. The harvest date was October 1st in both 2016 and 2017. The plant growth stages are given in Table 1. The fields were flood irrigated three or four times during the heading and filling stages starting in late June or early July (Table 2).

Precipitation, air temperature, relative humidity, sunshine duration and wind speed were collected from the weather station on the experimental station. The reference evapotranspiration (ET_0) was calculated based on the FAO-Penman-Monteith equation with the daily meteorological data (Allen et al., 1998). Precipitation and ET_0 during crop growth stage were showed in Fig. 2. The soil moisture was monitored daily in the top 90 cm using Hydra Probe Soil Sensors (Stevens Water Monitoring System Inc., Portland, OR, USA) installed in both experiment

Hydrol. Earth Syst. Sci. Discuss., https://doi.org/10.5194/hess-2018-581
Manuscript under review for journal Hydrol. Earth Syst. Sci.
Discussion started: 11 December 2018

fields. Soil moisture was measured at 5 depths: 0-10 cm, 10-30 cm, 30-50 cm, 50-70 cm, and 70-90 cm. The sensors were connected to data loggers and downloaded via wireless transmission. Calibration was conducted by oven drying soil samples (Wang et al., 2018; Gao et al., 2017a). The groundwater depth was measured by piezometers (HOBO Water Level Logger-U20, Onset, Cape Cod, MA, USA) recorded at 30 min intervals.

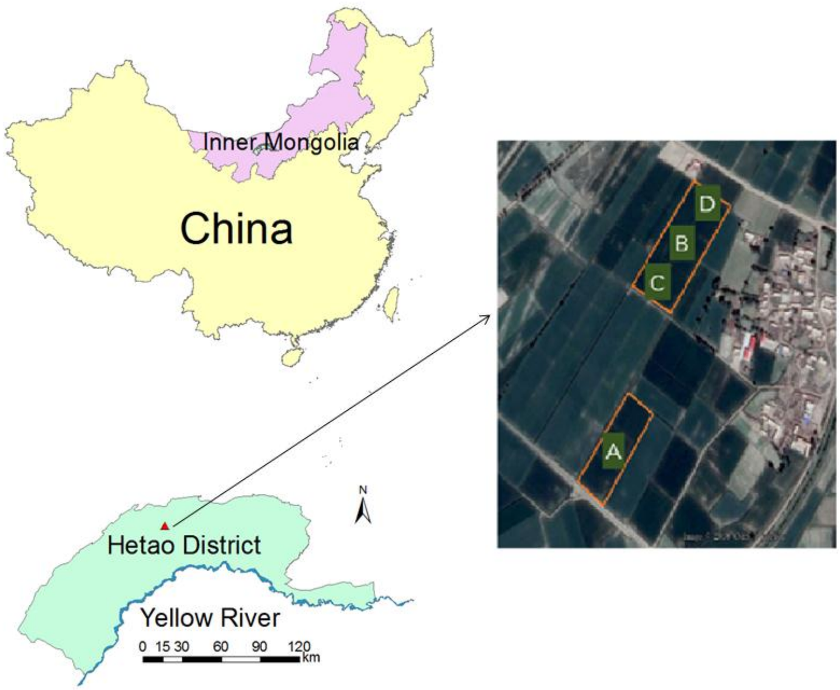

Figure. 1 Location of the field experiment in Hetao irrigation district. The blue line is the Yellow River.

Table 1

Crop growth stage in 2016 and 2017 for corn growth on the Fenzidi experimental fields in the Hetao district

Year\Growth stage	seeding	jointing	heading	filling	maturing	harvesting
2016	24-Apr	25-May	16-Jul	6-Aug	3-Sep	1-Oct
2017	13-May	11-Jun	18-Jul	8-Aug	5-Sep	1-Oct

Hydrol. Earth Syst. Sci. Discuss., https://doi.org/10.5194/hess-2018-581
Manuscript under review for journal Hydrol. Earth Syst. Sci.
Discussion started: 11 December 2018

Table 2

Irrigation scheduling carried out at Fenzidi experimental fields in 2016 and 2017

Year	Field	Irrigation events	Date	Irrigation depth(mm)
2016	A	First	July 13	115
		Second	July 26	86
		Third	August 8	122
	B	First	June 23	57
		Second	July 13	119
		Third	July 26	86
		Fourth	August 8	122
2017	C	First	July 13	153
		Second	July 23	104
		Third	August 9	134
	D	First	July 13	165
		Second	July 23	107
		Third	August 9	128

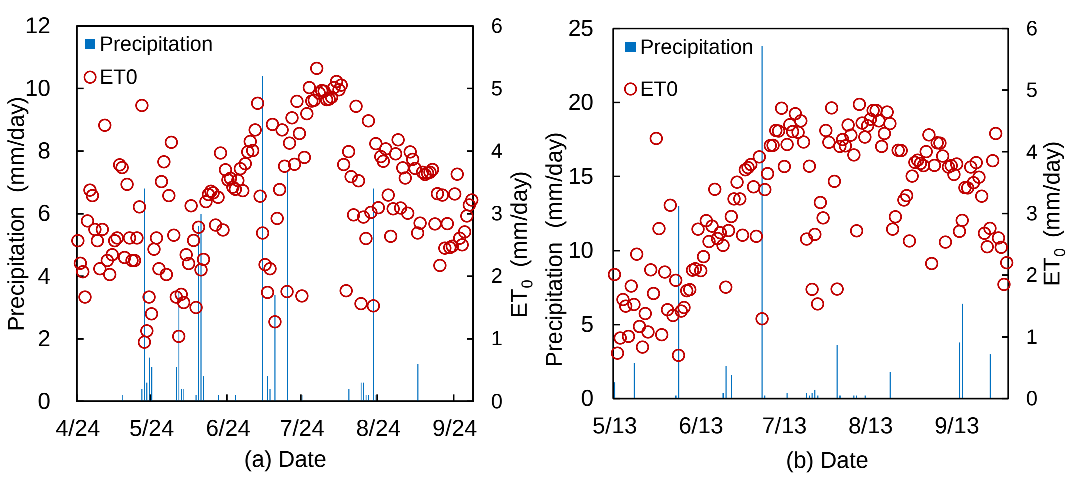

Figure. 2 Daily reference evaporation, ET0, and precipitation during crop growth period in (a) 2016 and (b) 2017

Soil samples were collected in rings from the same five layers where moisture contents were measured and used for determining soil physical properties including field capacity (θ_{fc}), saturated soil moisture (θ_s), dry bulk density (ρ), and saturated hydraulic conductivity (K_s) (Table 3). For Fields A, B, C and D, the saturated hydraulic conductivity was measured by the constant head method. Field capacity was measured at 33 kPa and bulk density was determined by oven drying and dividing by the volume of the ring. Soil texture of Fields A and B were analyzed with the laser particle size analyzer (Mastersizer 2000, Malvern Instruments Ltd. United Kingdom) in the laboratory and are shown in Table 4. The soils vary from silty loam to silty clay loam.

Table 3

Hydrological characteristic parameters of the Fenzidi experimental fields

Year	Field	Soil depth (cm)	θ_{fc} (cm^3/cm^3)	θ_s (cm^3/cm^3)	Ks (cm/d)	ρ (g/cm^3)
2016	A	0-10	0.31	0.47	11.65	1.47
		10-30	0.31	0.47	11.65	1.47
		30-50	0.32	0.51	48.71	1.36
		50-70	0.39	0.44	17.48	1.39
		70-100	0.41	0.44	40.54	1.45
	B	0-10	0.31	0.49	11.39	1.52
		10-30	0.31	0.49	11.39	1.52
		30-50	0.35	0.48	48.68	1.40
		50-70	0.40	0.49	11.06	1.42
		70-100	0.40	0.43	46.68	1.42
2017	C	0-10	0.36	0.42	5.18	1.52
		10-30	0.36	0.46	5.18	1.52
		30-50	0.35	0.47	11.92	1.38
		50-70	0.42	0.48	4.41	1.37
		70-100	0.21	0.47	6.23	1.69
	D	0-10	0.37	0.41	4.69	1.44
		10-30	0.37	0.45	4.69	1.44
		30-50	0.39	0.45	6.81	1.42
		50-70	0.42	0.46	10.86	1.42
		70-100	0.29	0.42	10.86	1.76

Note: θ_{fc} is the soil water content at 33 kPa, θ_s is the saturated soil water content, K_s is the saturated hydraulic conductivity, ρ is the bulk density, ψ_h is the bubbling pressure.

Table 4

Soil texture of the Field A and B

Site	Depth (cm)	Soil type	Sand (50-2000μm)	Silt (2-50μm)	Clay (0.01-2μm)
A	0-30	silty clay loam	0.05	0.75	0.2
	30-50	silty loam	0.22	0.7	0.08
	50-70	silty clay loam	0.03	0.8	0.17
	70-100	silty loam	0.39	0.57	0.04
B	0-30	silty loam	0.15	0.67	0.18
	30-50	silty loam	0.35	0.6	0.05
	50-70	silty clay loam	0.03	0.74	0.23
	70-100	silty clay loam	0.08	0.69	0.23

2.3 The Shallow Aquifer - Vadose Zone model

For shallow groundwater (less than 3.3 m deep), the matric potential is a function of depth under equilibrium conditions. Since the soil characteristic curve for each soil is the relationship of moisture content and matric potential, the moisture content is also a function of the depth of the water table under equilibrium conditions.

Soil characteristic curve

There are several formulations describing the soil characteristic curve (Bauters et al., 2000; Brooks and Corey, 1964; Gupta and Larson, 1979; Haverkamp and Parlange, 1986; van Genuchten, 1980); the van Genuchten and Brooks & Corey models are widely used in the hydrological and soil studies. Here, we selected the Brooks and Corey model for its simplicity.

The Brooks-Corey model can be expressed as (Gardner et al., 1970a; Gardner et al., 1970b; Mccuen et al., 1981; Williams et al., 1983).

$$S_e = \left(\frac{\varphi_m}{\varphi_b}\right)^{-\lambda} \qquad for\ |\varphi_m| > |\varphi_b| \qquad (1a)$$

$$S_e = 1 \qquad for\ |\varphi_m| \leq |\varphi_b| \qquad (1b)$$

in which S_e is the effective saturation θ is the volumetric moisture content, θ_s is the volumetric saturated moisture content, φ_b is the bubbling pressure (cm), φ_m is matric potential (cm), and λ is the pore size distribution index. The effective saturation is defined as

Hydrol. Earth Syst. Sci. Discuss., https://doi.org/10.5194/hess-2018-581
Manuscript under review for journal Hydrol. Earth Syst. Sci.
Discussion started: 11 December 2018

Hydrology and Earth System Sciences
Open Access
Discussions

$$S_e = \frac{\theta - \theta_d}{\theta_s - \theta_d} \tag{2}$$

in which θ is the volumetric moisture content, θ_s is the volumetric saturated moisture content, θ_d is the residual moisture content (all in cm^3/cm^3). Equation 2 can be simplified to the form by setting $\theta_d = 0$

$$S_e = \frac{\theta}{\theta_s} \tag{3}$$

For cases when the groundwater is close to the surface, under equilibrium conditions when the flow of water has stopped, the matric potential can be expressed as height above the water table. For our field experiment the bubbling pressure, φ_b, and the pore size distribution index, λ, in the Brooks and Corey model can be obtained through a trial and error procedure by using the measured moisture content and matric potential derived from the ground water depth after the field after an irrigation and equilibrium was reached.

2.3.1 Parameters based on soil characteristic curve

The soil of the crop root zone is divided into several soil layers and each soil layer has its specific soil characteristic curve. After a sufficiently large irrigation and rainfall event, the moisture content is at the equilibrium after the drainage stops. After such an event, the groundwater stays at the equilibrium moisture content as long as the evapotranspiration is less than upward flux from the groundwater.

Equilibrium moisture content

The equilibrium soil moisture content, θ_{equ}, in a layer can be determined by first replacing the matric potential in Eq (1a) by the matric potential of the layer $\varphi_m^{z,h}$ that is dependent of the depth of the groundwater and depth of the soil layer, z, e.g.

$$\varphi_m^{z,h} = h - z \tag{4}$$

where $\varphi_m^{z,h}$ is the matric potential under equilibrium moisture content at a depth z below the surface and h is the depth of the ground water below the surface

$$\theta_{eq}^{z,h} = \theta_s^z \left(\frac{h-z}{\varphi_b^z}\right)^{-\lambda} \qquad for \lceil h-z \rceil > |\varphi_b^z| \qquad (5a)$$

$$\theta_{eq}^{z,h} = \theta_s^z \qquad for \lceil h-z \rceil \le \lceil \varphi_b^z \rceil \qquad (5b)$$

where $\theta_{eq}^{z,h}$ is the equilibrium soil moisture at the depth z below the surface while the groundwater depth is h. Note that the superscripts *z* and *h* indicate the dependence on the distance from the soil surface, *z*, and the depth, *h*, of the groundwater table.

Drainable porosity

The drainable porosity, or specific yield, is defined as the amount of water drained from the soil for a unit decrease of the groundwater table when the soil moisture is at equilibrium. Thus, by subtracting the total moisture content at equilibrium in the profile at the initial water table depth and at the new position one unit lower, we obtain the drainable porosity. For example, the area between the orange and blue curve is the amount of water drained for a decrease in the water table from 130cm to 150cm (Fig.3).

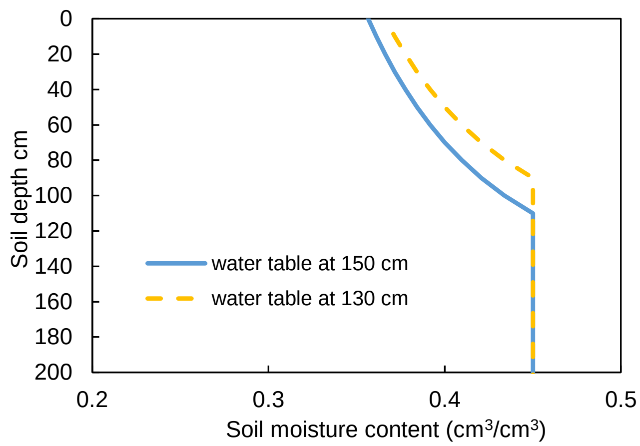

Figure. 3 Illustration of drainable porosity. The yellow and the blue line are the equilibrium moisture contents for the ground water depth at 130 and 150 cm, respectively. The area between the two lines represents the drained amount of water for the decrease of groundwater table drained from the profile when the ground water decreases from 130 to 150 cm.

The total water content amount of the soil over a prescribed depth with a water table at depth *h* can be expressed as

$$W_{eq}^{h} = \sum_{j=1}^{n} L_j \overline{\left(\theta_{eq}^{z,h}\right)_j} \qquad (6)$$

Hydrol. Earth Syst. Sci. Discuss., https://doi.org/10.5194/hess-2018-581
Manuscript under review for journal Hydrol. Earth Syst. Sci.
Discussion started: 11 December 2018

Hydrology and Earth System Sciences
Discussions

where $\overline{\theta_{eq}^{z,h}}$ is the average equilibrium moisture content of layer j for h taken at the midpoint of the layer, n is the number of layers in the profile, L_j is the height of soil layer j. And the drainable porosity, μ^h, with the groundwater at depth h, can simply be found as

$$\mu^h = \frac{W_{eq}^{h-\Delta h} - W_{eq}^{h+\Delta h}}{2\Delta h} \qquad (7)$$

where Δh =0.5L_j.

2.3.2 Calculating fluxes in the soil

The model accounts for the downward flux due to the irrigation and rainfall, evapotranspiration by plants and soil, and upward flux from the groundwater to satisfy some or all the evapotranspiration demand by the crop and soil. There are sets of rules implemented in an Excel spreadsheet to calculate the fluxes.

Evaporation

1. Evaporation is always at the maximum rate when the plant canopy is closed. The maximum rate is less than the potential rate because the soil water is saline. In addition, the evaporation is further reduced when the canopy is not closed.
2. (a) On days without rain or irrigation, the evaporation lowers the water table and the moisture content in the soil decreases due to upward movement of water to the plant roots and soil surface.

   (b) On days with rain or irrigation, the potential evaporation is subtracted from the irrigation and/or rainfall and water moves downward.

Upward flux from groundwater

3. The upward flux from the groundwater, U_g^h, is either limited by the potential evaporation or the maximum flux of groundwater. The maximum flux, $U_{g,max}^h$, depends on the depth of the groundwater, the type of soil characteristic curve, and the condition at the surface (Gardner, 1958). These equations have an exponential form (Gardner, 1958; Yang et al., 2011; Zammouri, 2001),

$$U_{g,max}^h = \frac{a}{e^{bh} - 1} \quad \text{for } U_g^h \leq ET_p \qquad (8)$$

   where a and b are constants and ET_p is the potential evapotranspiration. The upward flux from the groundwater can be written as:

$$U_g^h = \min\left(ET_p\, , U_{g,max}^h\right) \qquad (9)$$

On days without rain or irrigation, the soil moisture content is calculated by taking the difference of the equilibrium moisture content associated with the change in depth of groundwater. If in addition the upward flux is less than and evapotranspiration, the difference between the upward and the evapotranspiration is extracted out of the root zone according to a predermined distribution,r_j, e.g.,

$$\overline{(\theta^{z,h,t})}_j = \overline{(\theta^{z,h,t-\Delta t})}_j + \overline{(\theta_{eq}^{z,h,t})}_j - \overline{(\theta_{eq}^{z,h,t-\Delta t})}_j - \frac{r_j\left(K_c ET_p - U_g^h\right)}{L_j} \quad (10)$$

Where $\overline{(\theta^{z,h,t})}_j$ is the average soil moisture content at time t of layer j, $\overline{(\theta_{eq}^{z,h,t})}_j$ is the average equilibrium soil moisture content of layer j when the groundwater depth is h at time t, K_c is a reduction factor of the potential evaporation for saline soil water and canopy and r_j is the root function that determines the portion of the evaporation is taken up by the roots in layer j. The value z is taken at the midpoint of layer j. The time t is expressed in days and time, t-Δt, is the previous day.

The downward flux

4. The rules for downward flux on days with the effective rain and/or irrigation are relatively simple. If the net flux at the surface (irrigation plus rainfall minus actual evaporation) is greater than needed to bring the soil up to equilibrium moisture content, the groundwater will be recharged and increase in depth and the moisture content will be equal to the equilibrium moisture content at the new depth.
5. When the groundwater is not recharged, the following water balance will be calculated: the rainfall and the irrigation are added to first layer. This layer will be brought up to the equilibrium moisture content and the remaining water fills up the next layer to the equilibrium moisture content and so on. The calculations can be expressed as follows:

$$\overline{(\theta^{z,h,t})}_j = min\left[\overline{(\theta_{eq}^{z,h,t})}_j, \overline{(\theta^{z,h,t-\Delta t})}_j + \frac{R_{j-1}\Delta t}{L_j}\right] \quad (1\,1)$$

where for $j \geq 2$, R_{j-1} is the flux from the layer above and equals

$$R_{j+1} = R_j - \frac{\left(\overline{(\theta_{eq}^{z,h,t})}_j - \overline{(\theta^{z,h,t-\Delta t})}\right)L_j}{\Delta t} \quad (12)$$

For j=1, R_1 is equal to the rainfall plus the irrigation amounts minus potential evaporation

Groundwater table depth

6. The net change in groundwater depth, Δh, can be calculated on days without rainfall or irrigation as

Hydrol. Earth Syst. Sci. Discuss., https://doi.org/10.5194/hess-2018-581
Manuscript under review for journal Hydrol. Earth Syst. Sci.
Discussion started: 11 December 2018

Hydrology and Earth System Sciences
Open Access
Discussions

$$\Delta h = \frac{U_g^h}{\mu^h} \qquad (13a)$$

and days with rain or irrigation as

$$\Delta h = -\frac{R_5}{\mu^h} \qquad (13b)$$

where the upward flux, U_g^h, is calculated with Eq 9, the percolation of the bottom layer R_5 with Eq 12 and the drainable porosity, μ^h with Eq 7. When the groundwater is close to the surface, the drainable porosity is zero. This would make the change in groundwater infinite. Thus, we limited the maximum decrease in groundwater after the irrigation event to be 10-20 cm based on field observations.

2.3.3 Model calibration and validation

The soil moisture contents were measured from May 30th to September 25th in 2016 and 2017. Groundwater depth was observed from June 13th to September 26th in 2016 and 2017. For the convenience of simulation, the period of June 13th to September 25th was set as the simulation period. Model calibration and validation were carried out with data collected during the 2016 and 2017 growing seasons, respectively. Soil moisture content of the top 90 cm (0-10 cm, 10-30 cm, 30-50 cm, 50-70 cm, 70-90 cm) and the groundwater depth were simulated for model calibration and validation.

The statistical indicators including the mean relative error (*MRE*), the root mean square error (*RMSE*), the regression coefficient (*b*), the determination coefficient (R^2), and the regression slope were used to qualify the model fitting performance during the model calibration and validation. These indicators were defined as follows (Ren et al., 2016):

$$MRE = \frac{1}{N}\sum_{i=1}^{N}\frac{(P_i - O_i)}{O_i} * 100\% \qquad (14)$$

$$RMSE = \sqrt{\frac{1}{N}\sum_{i=1}^{N}(P_i - O_i)^2} \qquad (15)$$

$$b = \frac{\sum_{i=1}^{N} O_i * P_i}{\sum_{i=1}^{N} O_i^2} \qquad (16)$$

$$R^2 = \left[\frac{\sum_{i=1}^{N} (O_i - \bar{O})(P_i - \bar{P})}{\left[\sum_{i=1}^{N} (O_i - \bar{O})^2 \right]^{0.5} \left[\sum_{i=1}^{N} (P_i - \bar{P})^2 \right]^{0.5}} \right]^2 \qquad (17)$$

where N is the total number of observations, O_i and P_i are the ith observed and predicted values ($i=1, 2,\ldots, N$), and $\bar{O}$ and $\bar{P}$ are the mean observed values and mean predicted values, respectively. For *MRE* and *RMSE*, the values closest to 0 indicates good model predictions. For *b* and R^2, the values closest to 1 indicates good model predictions.

3 Results

In this section, we present first the 2016 and 2017 experimental observations of the Fenzidi experimental fields in the Hetao irrigation district (Fig.1). This is followed by the calibration and validation of the Shallow Aquifer-Vadose Zone Model of moisture content in each of the five layers and the groundwater table depth.

3.1 Results of the field experiment

The total precipitation at the experimental field during growing season was 62 mm in 2016 and 67 mm in 2017. The maximum daily rainfall was 23 mm in July 2017 (Fig. 2). The reference evapotranspiration varied between 1 mm/day to 5.5 mm/day and the total ET_0 was 517 mm and 442 mm in the growing seasons during 2016 and 2017, respectively (Fig.2). Daily observation consisted of soil moisture content at five soil depths up to 90 cm (blue spheres, Fig.4) and groundwater depth (blue spheres, Fig.5) for Fields A and B in 2016 and Fields C and D in 2017.

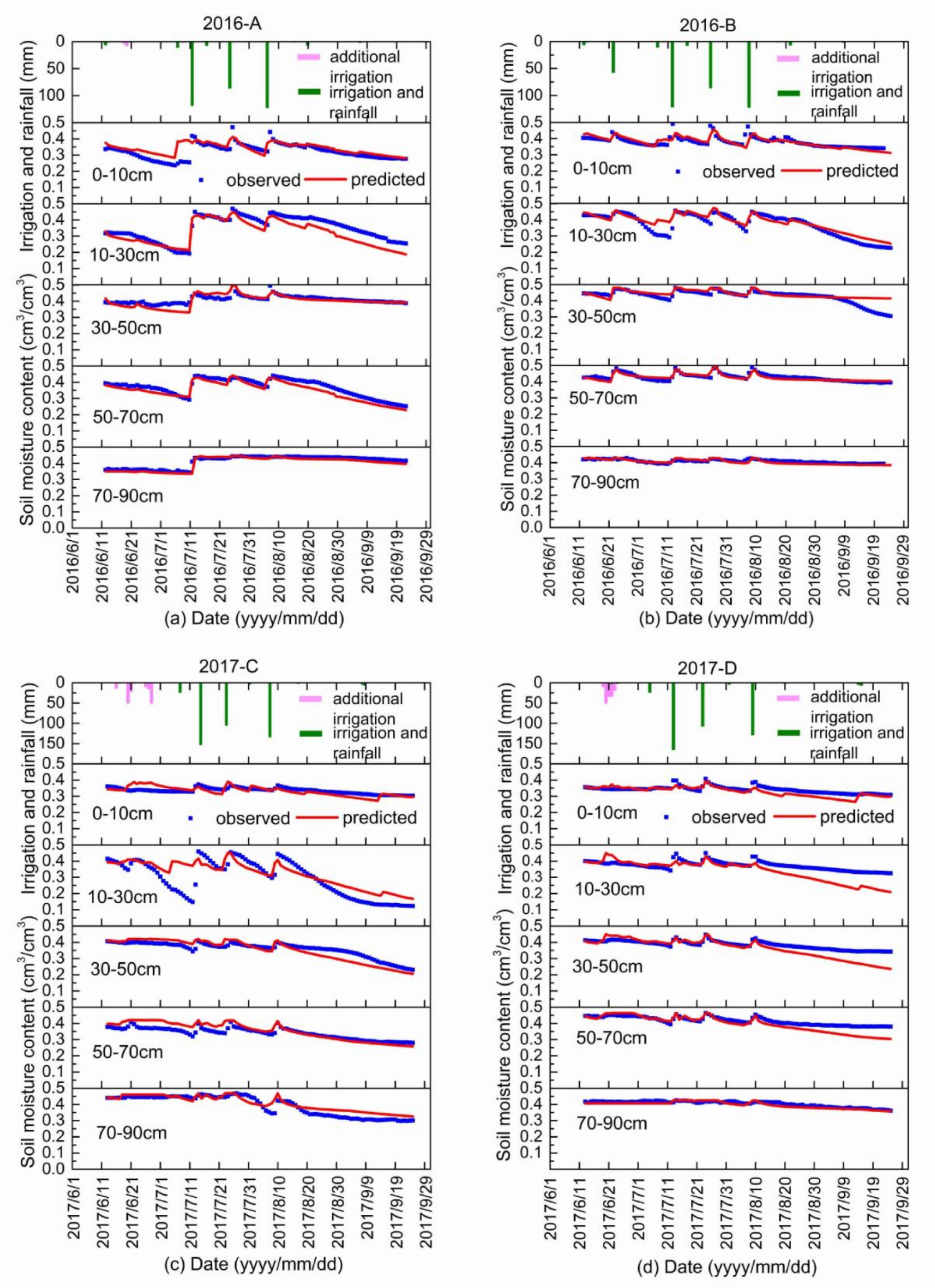

Figure. 4 Simulated and observed soil moisture content for five soil depths during the growing period for the Fenzidi experimental fields in the Hetao irrigation district: (a, b) calibration in 2016 and (c, d) validation in 2017.

Hydrol. Earth Syst. Sci. Discuss., https://doi.org/10.5194/hess-2018-581
Manuscript under review for journal Hydrol. Earth Syst. Sci.
Discussion started: 11 December 2018

Hydrology and Earth System Sciences
Open Access
Discussions

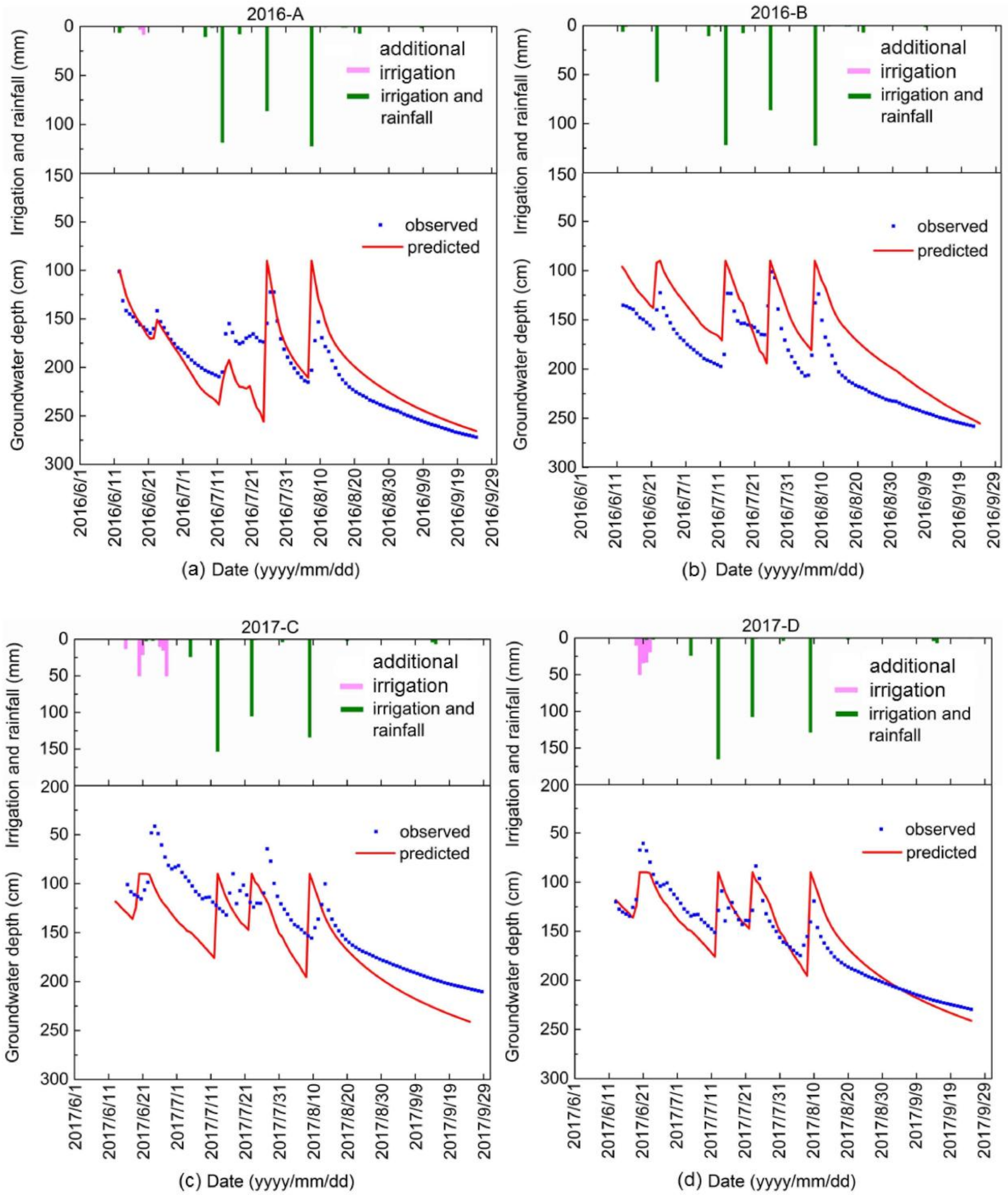

Figure.5 Simulated and observed groundwater depth during the growing period for the Fenzidi experimental fields in the Hetao irrigation district: (a,b) calibration in 2016 and (c,d) validation in 2017. (Notes: Additional irrigation means the irrigation recharge from the adjacent field which leads to the water table rise and was not planned).

3.1.1 Groundwater observations

In 2016, the groundwater depth was generally more than 100 cm except during the last two irrigation events on Field B when it reached a depth of 72 cm for one or two days (Fig. 5). In 2017, groundwater tables were slightly closer to the surface than in 2016, especially in Field D. The minimum groundwater depth was 61 cm on June 21, 2017 in Field D after an irrigation event.

In general, groundwater rose during an irrigation event and then decreased slowly due to upward movement of water to the plant roots to meet the transpiration demand. However, in the beginning of the growing season, we can see that the water table increased without an irrigation event. This occurred on Field A on June 24, 2016 and Fields C and D on June 20, 2017 (Fig. 5). This is curious and could be due to water originating from irrigation in a nearby field.

The water table at the end of the period of observation on September 25, 2016 is approximately 2 m deep, while on June 15, 2017, the depth decreased to around 125 cm. This is due to an irrigation application after the crops were harvested to leach the salt from the surface to deeper in the profile bringing the water table up to near the surface. Evaporation during the winter is small but sufficient to bring the water table down. There was also a rainfall event on June 5, 2017 of 13 mm (Fig. 2) before the water table was measured, increasing the water level.

3.1.2 Soil Moisture

Moisture contents are shown for the five layers and the two fields for 2016 and 2017 in Fig. 4. The moisture contents were near saturation when irrigation water was added and subsequently decreased (Fig. 4). For example, the soil moisture content changed in the 0-10 cm layer from 0.26 cm^3/cm^3 to 0.42 cm^3/cm^3 after the irrigation on July 13, 2016 in Field A and then gradually decreased to 0.34 cm^3/cm^3. The moisture content decreased faster in the 10-30 cm depth than at any other depth for Fields A, B and C but not for Field D. The moisture content in Field A also showed a decrease at the 50-70 cm depth. For all plots, the moisture content at the 70-90 cm depth stayed nearly constant and only decreased at the growing season when the water table decreased below the 150 cm depth (Fig. 5). In Field A, the initial moisture content when the observation started was less than saturation and then after the first irrigation, remained close to the saturated moisture content.

It is interesting that while the soil profile was saturated (Fig. 4), the groundwater table was between 75-100 cm (Fig. 5). Before equilibrium moisture content was reached the water table was likely near the surface during the irrigation event. Because the drainable porosity was extremely small, even a minimum amount of evaporation or

Hydrol. Earth Syst. Sci. Discuss., https://doi.org/10.5194/hess-2018-581
Manuscript under review for journal Hydrol. Earth Syst. Sci.
Discussion started: 11 December 2018

Hydrology and Earth System Sciences
Open Access
Discussions

drainage would cause the water table to decrease to roughly the height of the capillary fringe equal to the bubble pressure, φ_b, in Eq. 5.

3.1.3 Soil characteristic curve

In 2016 and 2017, the observed reduced moisture contents were plotted versus the height above the water table for the five soil layers of the two field sites in Fig. 6. These plots were used to define the soil characteristic curves which were of critical importance in simulating the moisture contents.

To define the soil characteristic curve, the Brooks-Corey equation (Eq. 1) was fitted through the points closest to saturation at each matric potential representing the equilibrium conditions after an irrigation event. The fitted parameter values are shown in Table 5. Points to the left of the soil characteristic curve are a result of evaporation drying out the soil when the upward movement of water was insufficient to replenish the moisture content in these layers and thus matric potential and ground water depth were not in equilibrium. In addition, the few points to the right indicate the soil moisture was greater than the equilibrium moisture content. Many of the outlier soil moisture contents occurred in the layer from 0-10 cm indicating that the soil was still draining after a rainfall event shortly before the measurements. Thus, the soil was not at the equilibrium moisture content.

The saturated moisture contents in Table 5 agree in general with the one measured in Table 1 but are not exact. This is not a surprise as the alluvial soil deposited by the rivers with layers vary over short distances. The variation within the field was also obvious from the soil's physical measurements. Fields C and D are within Field B. The soil's physical properties of the various layers (Table 4) were not the same for the three sites, clearly showing the variability within the field.

Generally, large values of pore size index coefficient λ are for sandy soils and lower values are for clay soils (Bahmani and Bayram, 2018). We find this to be true for our site: for example, in Field A, the λ=0.23 corresponds to a sandy layer with only 8% clay in the 30-50 cm layer (Tables 4 and 5). In the 70-90 cm layer of Field B, the λ=0.07 corresponds with the clay layer of 23% clay. In addition, bubbling pressure, φ_b, are greater for soils with a large clay content (Bahmani and Bayram, 2018). This is demonstrated for Field A in the 10-30 cm layer where the bubbling pressure of 75 cm corresponded with the clay layer of 20% clay. However, the correspondence between Tables 4 and 5 is not always perfect. This is especially obvious for the layer of 70-90 cm in Field A where the values in Table 5 clearly indicates that the soil has a dense clay layer; however, the soil description in Table 4 shows that the soil is 39% sand. This is due to the alluvial deposition patterns with changes in soil texture over short distances as mentioned before.

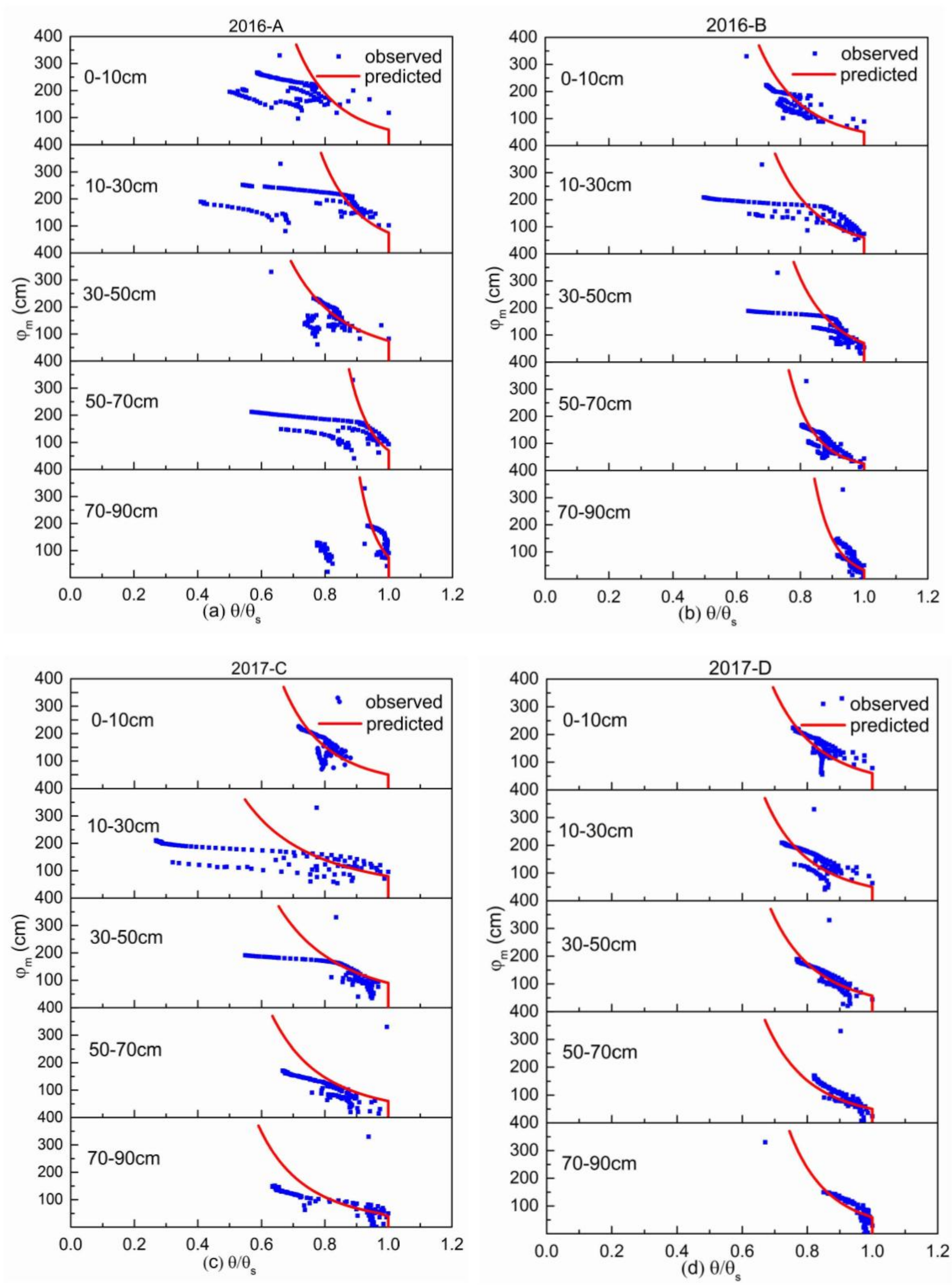

Figure.6 Soil characteristic curve of the four experiment fields for the Fenzidi experimental fields. The red line is the fit with the Brooks and Corey equation.

Table 5

Fitted Brooks and Corey parameters for the soil characteristic curve

Soil depth	Lamda(λ)				bubbling pressure (φ_b)cm				saturated moisture content (cm^3/cm^3)			
Field	A	B	C	D	A	B	C	D	A	B	C	D
0-10	0.18	0.2	0.2	0.2	55	50	50	60	0.47	0.49	0.42	0.41
10-30	0.15	0.18	0.17	0.2	75	60	70	50	0.47	0.48	0.46	0.45
30-50	0.23	0.15	0.25	0.2	75	70	50	57	0.51	0.48	0.47	0.45
50-70	0.08	0.1	0.25	0.2	70	25	30	50	0.44	0.49	0.48	0.46
70-90	0.06	0.07	0.3	0.16	75	33	45	59	0.44	0.43	0.47	0.42

3.2 Modeling results

Relatively few parameters can be calibrated in the Shallow Aquifer-Vadose Zone Model. These are the crop coefficients K_c value, the two groundwater parameters and the root function.

3.2.1 Calibration of the parameters related to moisture content

The first step in the calibration was to fit the K_c value from the water balance. From the moisture contents and the groundwater depth, we can calculate approximately the amount of water lost to evaporation. By comparing these values to the reference evaporation calculated with the Penman-Monteith equation, we found that initially during the early stages the crop coefficient was 0.3 until the filling stage and then increased to 0.7 during the filling stage to maturing stage (Table 6). These values are in accordance with the findings of (Katerji et al., 2003) that salinity reduces the evaporation. Moreover, according to FAO (1998), K_c values for early growth stages are 0.3 and K_c=0.7 for soils with median salinity (Allen et al., 1998).

The second step was calibrating the moisture content by adapting the root function indicating from what layers the water was taken up. Calibration was done manually by trial and error. We found that we could use the same root function for Fields A, B, C, and D (Table 6). The calibrated soil moisture contents of the five soil layers for the two fields are in general in agreement with the measured values in 2016 (Fig 4a, b) with coefficient of determination R^2 ranging between 0.48 to 0.94 with slopes of around one; the mean relative error (*MRE*) between -0.09 and 0.07 and the root mean square error (*RMSE*) varied from 0.01 to 0.04 cm^3/cm^3 for the five layers (Table 7-1). Finally, the

Hydrol. Earth Syst. Sci. Discuss., https://doi.org/10.5194/hess-2018-581
Manuscript under review for journal Hydrol. Earth Syst. Sci.
Discussion started: 11 December 2018

parameters behaved physically realistic as water was extracted from shallow layers when the groundwater was close to the surface and from the deeper layers when the groundwater and the associated capillary fringe went down.

Table 6

Calibrated parameter values of the Vadose Zone Shallow Aquifer model

Items		Date	Calibrated value
Crop parameter,Kc		June 13-July 14	0.3
		July 15-September 25	0.7
Root function, r_j	0-10cm	June 13-August 7	0.2
		August 8-September 3	0.1
		September 4-October 1	0.1
	10-30cm	June 13-August 7	0.4
		August 8-September 3	0.4
		September 4-October 1	0.4
	30-50cm	June 13-August 7	0.3
		August 8-September 3	0.3
		September 4-October 1	0.3
	50-70cm	June 13-August 7	0.1
		August 8-September 3	0.2
		September 4-October 1	0.1
	70-90cm	June 13-August 7	0
		August 8-September 3	0
		September 4-October 1	0.1
a		Field A	80
b			0.021
a		Field B, C ,D	110
B			0.025

3.2.2. Validation of the parameters related to moisture content

The moisture contents predicted by the Shallow Aquifer-Vadose Zone Model were validated with the 2017 data on Fields C and D. Although the validation statistics of the five layers were slightly less good than for calibration in Table 7, the overall fit was still good as shown in Fig. 4c, d. The determination coefficient varied between 0.39 and 0.90. The *MRE* varied between -0.09 and 0.19, and the mean *RMSE* range was from 0.01 to 0.07 cm^3/cm^3 for the five soil layers (Table 7-2).

3.2.3 Calibration of the parameters related groundwater depth

The final step was to calibrate the groundwater table coefficients with the 2016 data for both fields. We found that for fields not in the same location (e.g., A, B) the subsurface was sufficiently different so that the same set of parameters could not be used (Table 6). The difference between the calibrated parameters for the two fields was small (Table 6). The measured and simulated groundwater depth were in good agreement with the chosen set of parameters (Fig. 5a, b) with coefficient of determination R^2 being 0.67 for Field A and 0.85 for Field B with most slopes of the regression line of around 1 (Table 7-1). Only from July 15 to July 25 did the observed water table on Field B decrease slower than the simulated water table. This is likely related to the drainable porosity of the soil that was not known below 90 cm for which the soil characteristic curve was not measured. Other statistics showed the good fit as well (Table 7-1) with the mean relative error (*MRE*) is 0 for Field A and 0.02 for Field B; the root mean square error (*RMSE*) is 27 cm for Field A and 18 cm for Field B; the regression coefficient *b* is 0.98 for Field A and 1 for Field B.

Table 7-1

Model statistics for calibration of the Shallow Aquifer model in 2016 Mean relative error, MRE; root mean square error, RMSE; Regression slope; Coefficient of determination, R2; Regression coefficient, b.

Calibration (2016)							
		Soil moisture content					Groundwater depth
		0-10cm	10-30cm	30-50cm	50-70cm	70-90cm	
A	MRE(%)	0.07	-0.09	-0.02	-0.06	-0.02	0.00
	RMSE	0.04	0.04	0.02	0.03	0.01	27
	Regression Slope	0.51	0.94	1.34	1.01	1.05	0.94
	R^2	0.49	0.84	0.72	0.92	0.94	0.67
	b	1.05	0.91	0.99	0.94	0.98	0.98
B	MRE(%)	-0.01	0.05	0.04	0.00	-0.01	0.02
	RMSE	0.02	0.03	0.03	0.01	0.01	18
	Regression Slope	0.93	0.72	0.37	0.76	1.14	0.82
	R^2	0.73	0.85	0.48	0.74	0.69	0.85
	b	0.99	1.03	1.03	0.99	0.99	1.0

Hydrol. Earth Syst. Sci. Discuss., https://doi.org/10.5194/hess-2018-581
Manuscript under review for journal Hydrol. Earth Syst. Sci.
Discussion started: 11 December 2018

Hydrology and Earth System Sciences
Open Access
Discussions

3.2.4 Validation of the parameters related groundwater depth

Since Fields C and D are in the same location as Field B, we used the same set of groundwater parameters for the three fields (Table 6). The resulting fit between observed and predicted daily groundwater depths for Fields C and D in 2017 was better than for the calibration in 2016 (Fig. 5c, d) with R^2 values of 0.84 for Field C and 0.86 for Field D (Table 7-2). In both cases, the slope of the regression line was close to 1. The other statistics indicated a good fit as well (Table 7-2) with the mean relative error (*MRE*) being -0.05 for Field C and -0.02 for Field D; the root mean square error (*RMSE*) is 19 cm for Field C and 17 cm for Field D; the regression coefficient *b* is 0.94 and 1 for Fields C and D, respectively. The general agreement between the measured and simulated groundwater depth suggests that the two parameters are adequate, and the model can be used as a tool to simulate the change of the groundwater depth.

Table 7-2

Model statistics for validation of the Shallow Aquifer model in 2017- Mean relative error, MRE; root mean square error, RMSE; Regression slope; Coefficient of determination, R2; Regression coefficient, b.

Validation (2017)							
		Soil moisture content					Groundwater depth
		0-10cm	10-30cm	30-50cm	50-70cm	70-90cm	
C	MRE(%)	-0.01	0.19	-0.03	0.04	0.05	-0.05
	RMSE	0.02	0.07	0.03	0.03	0.03	19
	Regression Slope	1.03	0.57	1.38	1.49	0.70	1.0
	R^2	0.39	0.65	0.87	0.88	0.88	0.84
	b	0.99	1.03	0.99	1.05	1.03	0.94
D	MRE(%)	-0.04	-0.09	-0.06	-0.05	-0.02	0.01
	RMSE	0.02	0.05	0.04	0.03	0.01	17
	Regression Slope	1.11	1.92	2.24	1.89	1.02	1.1
	R^2	0.62	0.68	0.90	0.90	0.83	0.86
	b	0.96	0.92	0.95	0.96	0.98	1.0

4 Discussion

In this manuscript, a novel model was developed for irrigation systems where the groundwater is close to the surface. The model uses the soil characteristic curve to derive the drainable porosity and to predict the moisture contents in the soil. It is based on a less often used definition of field capacity (or equilibrium moisture content as it is called in this manuscript) based on the observation that the flow stops when the hydraulic gradient is zero. In other words, the system is in equilibrium when the sum of the matric potential and the gravity potential is constant. Thus, when we chose the groundwater level as the reference point for the gravity potential, the matric potential is equal to the height above the groundwater. This is different from other application of Darcy's law where the groundwater is below 3.3 m. In these cases, groundwater movement stops when the conductivity becomes negligible at 33 kPa or 3.3 m in head units.

In general, this model simulated the soil moisture content in each soil layer well, certainly when compared to other models that attempted the soil moisture contents in the Yellow River basin such as North China Plain (Kendy et al., 2003) and the Hetao Irrigation District by Gao et al (2017b). Our simulation results suggest that the reduction factor of the potential evaporation for soil saline K_c and root function parameters, together with the information of the soil characteristic curves, can be used to adequately predict the soil moisture content. To predict the groundwater depth, two additional parameters are needed for the exponential function that defines the upward movement of groundwater.

The simulations, together with the observed data, indicates that information about the soil is very important to obtain the exact moisture content in the soil. However, generalized soil characteristic curves for each soil type can be used in the simulation and will not result in great differences in water use by plants since percolation to deeper layers was negligible and thus the only loss of water was by evaporation independent of the soil moisture content.

Finally, in the simulations we did not consider the influence of crop type and the influence of crop growth on soil moisture and groundwater depth. It would be of interest to investigate in future work whether the simulations would be improved by considering the dynamic crop characteristics during the growing season (Singh et al., 2018; Talebizadeh et al., 2018). A mature crop model, such as the EPIC model (Williams et al., 1989) that needs relative few parameters, will certainly help to predict the crop yield but might not change the water use predictions.

Hydrol. Earth Syst. Sci. Discuss., https://doi.org/10.5194/hess-2018-581
Manuscript under review for journal Hydrol. Earth Syst. Sci.
Discussion started: 11 December 2018

5 Conclusions

A novel vadose zone model for an irrigated area with a shallow aquifer was developed to simulate the fluctuation of groundwater depth and soil moisture during the crop growth stage in the shallow groundwater district. The model was calibrated and validated using two years of experimental field data. Using meteorological data and few soil hydraulic parameters related to the soil characteristic curve and upward capillary movement, the soil water content and groundwater can be simulated on daily time step. This model is simplified, so it can be used for management purposes.

Data availability: The observed data used in this study are not publicly accessible. These data have been collected by personnel the College of Water Resources and Civil Engineering, China Agricultural University, with fund from various cooperative sources. If anyone would like to use these data, they should contact Zhongyi Liu, Xingwang Wang and Zailin Huo to obtain permission.

Competing interests: The authors declare that they have no conflict of interest.

Acknowledgements: This study was supported by National Key Research and Development Program of China (2017YFC0403301) and the National Natural Science Foundation of China (No. 51639009, 51679236). Peggy Stevens helped greatly with polishing the English. We thank Xingwang Wang who helped in collecting field data.

References:

Abbott, M.B., Bathrust, J.C., Cunge, J.A., O'Connell, P.E., and Rasmussen, J.: An introduction to the European Hydrological System — Systeme Hydrologique Europeen, "SHE", 2: Structure of a physically-based, distributed modelling system. J. Hydrol., 87:61-77, https:// doi.org/10.1016/0022-1694(86)90115-0. 1986.

Alcamo, J., Florke, M., and Marker, M.: Future long-term changes in global water resources driven by socio-economic and climatic changes. Hydrolog Sci J., 52:247-275, https:// doi.org/ 10.1623/hysj.52.2.247. 2007.

Allen, R.G., Pereira, L.S., Raes, D., and Smith, M.: Crop evapotranspiration. Guidelines for computing crop water requirements-FAO Irrigation and Drainage Paper 56, FAO, Rome. 1998.

Bahmani, O., and Bayram, M.: Investigating the hydraulic conductivity and soil characteristics under compaction and soil texture and performances as landfill liner. Arab J Geosci., 11(16): 453. https:// doi.org/10.1007/s12517-018-3817-7. 2018.

Bauters, T.W.J., Steenhuis, T.S., Dicarlo, D.A., Nieber, J.L., Dekker, L.W., Ritsema, C.J., Parlange, J.Y., and Haverkamp, R.: Physics of water repellent soils. J. Hydrol., SI: 233-243. 2000.

Beven, K.J., and Kirkby, M.J.: A physically based, variable contributing area model of basin hydrology. Hydrolog Sci J., 24:43-69. https:// doi.org/10.1080/02626667909491834. 1979.

Brooks, R.H., and Corey, A.T.: Hydraulic properties of porous media, Hydrology Paper 3. Colorado State University. Fort Collins, Colorado, 37pp, 1964.

Hydrol. Earth Syst. Sci. Discuss., https://doi.org/10.5194/hess-2018-581
Manuscript under review for journal Hydrol. Earth Syst. Sci.
Discussion started: 11 December 2018

Hydrology and Earth System Sciences
Open Access
Discussions

Chen, C., Wang, E., and Yu, Q.: Modelling the effects of climate variability and water management on crop water productivity and water balance in the North China Plain. Agr. Water Manage., 97:1175-1184. https:// doi.org/10.1016/j.agwat.2008.11.012. 2010.

Du, C., Yu, J., Wang, P., and Zhang, Y.: Analysing the mechanisms of soil water and vapour transport in the desert vadose zone of the extremely arid region of northern China. J. Hydrol, 558:592-606. https:// doi.org/ 10.1016/j.jhydrol.2017.09.054. 2018.

Feng, Z., Wang, X., and Feng, Z.: Soil N and salinity leaching after the autumn irrigation and its impact on groundwater in Hetao Irrigation District, China. Agr. Water Manage., 71:131-143. https:// doi.org/ 10.1016/j.agwat.2004.07.001. 2005.

Flint, A.L., Flint, L.E., Kwicklis, E.M., Fabryka-Martin, J.T., and Bodvarsson, G.S.: Estimating recharge at Yucca Mountain, Nevada, USA: comparison of methods. Hydrogeol. J., 10:180-204. https:// doi.org/ 10.1007/s10040-001-0169-1. 2002.

Gao, X., Huo, Z., Qu, Z., Xu, X., Huang, G., and Steenhuis, T.S.: Modeling contribution of shallow groundwater to evapotranspiration and yield of maize in an arid area. Sci. Rep-UK 7. https:// doi.org/10.1038/srep43122. 2017a.

Gao, X., Huo, Z., Bai, Y., Feng, S., Huang, G., Shi, H., and Qu, Z.: Soil salt and groundwater change in flood irrigation field and uncultivated land: a case study based on 4-year field observations. Environ. Earth Sci., 73:2127-2139. https:// doi.org/10.1007/s12665-014-3563-4. 2015.

Gao, X., Bai, Y., Huo, Z., Xu, X., Huang, G., Xia, Y., and Steenhuis, T.S.: Deficit irrigation enhances contribution of shallow groundwater to crop water consumption in arid area. Agr. Water Manage., 185:116-125. https:// doi.org/ 10.1016/j.agwat.2017.02.012. 2017b.

Gardner, W.: Some study-state solutions of the unsaturated moisture flow equation with application to evaporation from a water table. Soil Sci., 85:228-232. 1958.

Gardner, W., Hillel, D., and Benyamini, Y.: Post-Irrigation Movement Soil Water 1. Redistribution. Water Resour. Res., 6:851-860. https:// doi.org/ 10.1029/WR006i003p00851. 1970a.

Gardner, W., Hillel, D., and Benyamini, Y.: Post-Irrigation Movement of Soil Water 2. Simultaneous Redistribution and Evaporation. Water Resour. Res., 6:1148-1153. https:// doi.org/ 10.1029/WR006i004p01148. 1970b.

Gardner-Outlaw, T., and Engelman, R.: Sustaining water, easing scarcity: A second update. Population Action International, Population and Environment Program .Washington, D.C.,18(2). 1997.

Gleeson, T., Befus, K.M., Jasechko, S., Luijendijk, E., and Cardenas, M.B.: The global volume and distribution of modern groundwater. Nat. Geosci., 9:161-167. https:// doi.org/10.1038/NGEO2590. 2016.

Guo, Y., and Shen, Y.: Agricultural water supply/demand changes under projected future climate change in the arid region of northwestern China. J. Hydrol, 540:257-273. https://doi.org/ 10.1016/j.jhydrol.2016.06.033. 2016.

Gupta, S., and Larson, W.: Estimating Soil Water Retention Characteristics From Particle Size Distribution, Organic Matter Percent, and Bulk Density. Water Resour. Res., 15:1633-1635. https:// doi.org/10.1029/WR015i006p01633. 1979.

Haverkamp, R., and Parlange, J.: Predicting the Water-Retention Curve from Particle-Size Distribution: 1. Sandy Soils Without Organic Matter1. Soil Sci., 142:325-339. https:// doi.org/10.1097/00010694-198612000-00001. 1986.

Hinrichsen, D., Henrylito D.T.: The Coming Freshwater Crisis is Already Here. Finding the Source: The Linkages Between Population and Water. Environmental Change and Security Program, Washington, DC, 26pp, 2002.

Hydrol. Earth Syst. Sci. Discuss., https://doi.org/10.5194/hess-2018-581
Manuscript under review for journal Hydrol. Earth Syst. Sci.
Discussion started: 11 December 2018

Hoang, L., Schneiderman, E.M., Moore, K.E.B., Mukundan, R., Owens, E.M., and Steenhuis, T.S.: Predicting saturation-excess runoff distribution with a lumped hillslope model: SWAT-HS. Hydrol. Process., 31:2226-2243. https:// doi.org/ 10.1002/hyp.11179. 2017.

Jasechko, S., and Taylor, R.G.: Intensive rainfall recharges tropical groundwaters. Environ. Res. Lett., 10:124015. https:// doi.org/10.1088/1748-9326/10/12/124015. 2015.

Kahlown, M., Ashraf, M., and Zia-Ul-Haq.: Effect of shallow groundwater table on crop water requirements and crop yields. Agr. Water Manage., 76:24-35. https:// doi.org/10.1016/j.agwat.2005.01.005. 2005.

Karimov, A.K., Hanjra, M.A., Šimůnek, J., and Abdurakhmannov, B..: Can a change in cropping patterns produce water savings and social gains: A case study from the Fergana Valley, Central Asia. J. Hydrol. Hydromech., 66:189-201. https:// doi.org/10.1515/johh-2017-0054. 2018.

Katerji, N., van Hoorn, J.W., Hamdy, A., and Mastrorilli, M.: Salinity effect on crop development and yield, analysis of salt tolerance according to several classification methods. Agr. Water Manage., 62:37-66. https:// doi.org/10.1016/S0378-3774(03)00005-2. 2003.

Kendy, E., Gérard-Marchant, P., Walter, M. T., Zhang, Y., Liu, C., and Steenhuis, T.S.: A soil-water-balance approach to quantify groundwater recharge from irrigated cropland in the North China Plain. Hydrol. Process., 17:2011-2031. https:// doi.org/10.1002/hyp.1240. 2003.

Li, C., Yang, Z., and Wang, X.: Trends of Annual Natural Runoff in the Yellow River Basin. Water Int., 29:447-454. https:// doi.org/10.1080/02508060408691807. 2004.

Liu, Z., Chen, H., Huo, Z., Wang, F., and Shock, C.C.: Analysis of the contribution of groundwater to evapotranspiration in an arid irrigation district with shallow water table. Agr. Water Manage., 171:131-141. https:// doi.org/10.1016/j.agwat.2016.04.002. 2016.

Luan, X., Wu, P., Sun, S., Wang, Y., and Gao, X.: Quantitative study of the crop production water footprint using the SWAT model. Ecol. Indic., 89:1-10. https:// doi.org/10.1016/j.ecolind.2018.01.046. 2018.

Luo, Y., and Sophocleous, M.: Seasonal groundwater contribution to crop-water use assessed with lysimeter observations and model simulations. J. Hydrol, 389:325-335. https:// doi.org/10.1016/j.jhydrol.2010.06.011. 2010.

Ma, Y., Feng, S., and Song, X.: A root zone model for estimating soil water balance and crop yield responsesto deficit irrigation in the North China Plain. Agr. Water Manage., 127:13-24. https:// doi.org/10.1016/j.agwat.2013.05.011. 2013.

Mccuen, R., Rawls, W., and Brakensiek, D.: Statistical Analysis of the Brooks-Corey and the Green-Ampt Parameters. Water Resour. Res., 17:1005-1013. https:// doi.org/10.1029/WR017i004p01005. 1981.

Mcdonald, M., and Harbaugh, A.: The history of MODFLOW. Groundwater 41:280-283. https:// doi.org/10.1111/j.1745-6584.2003.tb02591.x. 2003.

Merz, B., and Plate, E.: An analysis of the effects of spatial variability of soil and soil moisture on runoff. Water Resour. Res., 33: 2902-2922. https:// doi.org/10.1029/97WR02204. 1997.

Moiwo, J.P., Lu, W., Zhao, Y., Yang, Y., and Yang, Y.: Impact of land use on distributed hydrological processes in the semi-arid wetland ecosystem of Western Jilin. Hydrol. Process., 24:492-503. https:// doi.org/10.1002/hyp.7503. 2009.

Neitsch, S.L., Arnold, J.G., and Willams, J.R.: Soil and Water Assessment Tool-Theoretical Documentation - Version 2009. Grassland, Soil and Water Research Laboratory-Agricultural Research Service, Blackland

Hydrol. Earth Syst. Sci. Discuss., https://doi.org/10.5194/hess-2018-581
Manuscript under review for journal Hydrol. Earth Syst. Sci.
Discussion started: 11 December 2018

Hydrology and Earth System Sciences Discussions

Research Center-Texas AgriLife Research, Texas Water Resources Institute Technical Report No. 406, Texas A&M University System, College Station, Texas, USA, 2011.

Oki, T., and Kanae, S.: Global Hydrological Cycles and World Water Resources. Science, 313:1068-1072. https:// doi.org/10.1126/science.1128845. 2006.

Ren, D., Xu, X., Hao, Y., and Huang, G.: Modeling and assessing field irrigation water use in a canal system of Hetao, upper Yellow River basin: Application to maize, sunflower and watermelon. J. Hydrol, 532:122-139. https:// doi.org/10.1016/j.jhydrol.2015.11.040. 2016.

Ren, D., Xu, X., Engel, B., and Huang, G.: Growth responses of crops and natural vegetation to irrigation and water table changes in an agro-ecosystem of Hetao, upper Yellow River basin: Scenario analysis on maize, sunflower, watermelon and tamarisk. Agr. Water Manage., 199:93-104. https:// doi.org/10.1016/j.agwat.2017.12.021. 2018.

Rodriguez-Iturbe, I.: Ecohydrology: A hydrologic perspective of climate-soil-vegetation dynamics. Water Resour. Res., 36:3-9. https:// doi.org/10.1029/1999WR900210. 2000.

Singh, L.K., Jha, M.K., and Pandey, M.: Framework for Standardizing Less Data-Intensive Methods of Reference Evapotranspiration Estimation. Water Resour. Manag., 32:4159-4175. https:// doi.org/10.1007/s11269-018-2022-5. 2018.

Su, N., Bethune, M., Mann, L., and Heuperman, A.: Simulating water and salt movement in tile-drained fields irrigated with saline water under a Serial Biological Concentration management scenario. Agr. Water Manage., 78:165-180. https:// doi.org/10.1016/j.agwat.2005.02.003. 2005.

Sun, S., Wu, P., Wang, Y., Zhao, X., Liu, J., and Zhang, X.: The impacts of interannual climate variability and agricultural inputs on water footprint of crop production in an irrigation district of China. Sci. Total Environ., 444:498-507. https:// doi.org/10.1016/j.scitotenv.2012.12.016. 2013.

Talebizadeh, M., Moriasi, D., Gowda, P., Steiner, J.L., Tadesse, H.K., Nelson, A.M., and Starks, P.: Simultaneous calibration of evapotranspiration and crop yield in agronomic system modeling using the APEX model. Agr. Water Manage., 208:299-306. https:// doi.org/10.1016/j.agwat.2018.06.043. 2018.

van Genuchten, M.T.: A Closed-form Equation for Predicting the Hydraulic Conductivity of Unsaturated Soils. Soil Sci. Soc. Am. J., 44:892-898. https:// doi.org/10.2136 /sssaj1980.03615995004400050002x. 1980.

Venkatesh, B., Lakshman, N., Purandara, B.K., and Reddy, V.B.: Analysis of observed soil moisture patterns under different land covers in Western Ghats, India. J. Hydrol, 397:281-294. https:// doi.org/10.1016/j.jhydrol.2010.12.006. 2011.

Wang, E., and Smith, C.J.: Modelling the growth and water uptake function of plant root systems: a review. Aust. J. Agr. Res., 55:501. https:// doi.org/10.1071/AR03201. 2004.

Wang, H., Tetzlaff, D., and Soulsby, C.: Modelling the effects of land cover and climate change on soil water partitioning in a boreal headwater catchment. J. Hydrol, 558:520-531. https:// doi.org/10.1016/j.jhydrol.2018.02.002. 2018.

Wang, H., Zhang, L., Dawes, W.R., and Liu, C.: Improving water use efficiency of irrigated crops in the North China Plain - measurements and modelling. Agr. Water Manage., 48:151-167. https:// doi.org/10.1016/S0378-3774(00)00118-9. 2001.

Wang, Q., Huo, Z., Zhang, L., Wang, J., and Zhao, Y.: Impact of saline water irrigation on water use efficiency and soil salt accumulation for spring maize in arid regions of China. Agr. Water Manage., 163:125-138. https:// doi.org/10.1016/j.agwat.2015.09.012. 2016.

Hydrol. Earth Syst. Sci. Discuss., https://doi.org/10.5194/hess-2018-581
Manuscript under review for journal Hydrol. Earth Syst. Sci.
Discussion started: 11 December 2018

Hydrology and Earth System Sciences
Open Access
Discussions

Wang, X., Huo, Z., Guan, H., Guo, P., and Qu, Z.: Drip irrigation enhances shallow groundwater contribution to crop water consumption in an arid area. Hydrol. Process., 32:747-758. https:// doi.org/10.1002/hyp.11451. 2018.

Williams, J., Prebble, R., Williams, W., and Hignett, C.: The influence of texture, structure and clay mineralogy on the soil moisture characteristic. Aust. J. Soil Res., 21:15-32. https:// doi.org/10.1071/SR9830015. 1983.

Williams, J., Jones, C., Kiniry, J., and Spanel, D.: The EPIC Crop Growth Model. T. ASAE ,32:479-511. 1989.

Xu, X., Huang, G., Qu, Z., and Pereira, L.S.: Assessing the groundwater dynamics and impacts of water saving in the Hetao Irrigation District, Yellow River basin. Agr. Water Manage., 98:301-313. https:// doi.org/10.1016/j.agwat.2010.08.025. 2010.

Xu, X., Sun, C., Qu, Z., Huang, Q., Ramos, T.B., and Huang, G.: Groundwater Recharge and Capillary Rise in Irrigated Areas of the Upper Yellow River Basin Assessed by an Agro-Hydrological Model. Irrig. Drain., 64:587-599. https:// doi.org/10.1002/ird.1928. 2015.

Xue, J., Huo, Z., Wang, F., Kang, S., and Huang, G.: Untangling the effects of shallow groundwater and deficit irrigation on irrigation water productivity in arid region: New conceptual model. Sci. Total Environ., 619-620:1170-1182. https:// doi.org/10.1016/j.scitotenv.2017.11.145. 2018.

Yang, F., Zhang, G., Yin, X., Liu, Z., and Huang, Z.: Study on capillary rise from shallow groundwater and critical water table depth of a saline-sodic soil in western Songnen plain of China. Environ. Earth Sci., 64:2119-2126. https:// doi.org/10.1007/s12665-011-1038-4. 2011.

Yang, X., Chen, Y., Pacenka, S., Gao, W., Ma, L., Wang, G., Yan, P., Sui, P., and Steenhuis, T.S.: Effect of diversified crop rotations on groundwater levels and crop water productivity in the North China Plain. J. Hydrol., 522:428-438. https:// doi.org/ 10.1016/j.jhydrol.2015.01.010. 2015a.

Yang, X., Chen, Y., Pacenka, S., Gao, W., Zhang, M., Sui, P., and Steenhuis, T.S.: Recharge and Groundwater Use in the North China Plain for Six Irrigated Crops for an Eleven Year Period. Plos One 10:e0115269. https:// doi.org/10.1371/journal.pone.0115269. 2015b.

Yang, X., Chen, Y., Steenhuis, T.S., Pacenka, S., Gao, W., Ma, L., Zhang, M., and Sui, P.: Mitigating Groundwater Depletion in North China Plain with Cropping System that Alternate Deep and Shallow Rooted Crops. Front. Plant Sci., 8. https:// doi.org/ 10.3389/fpls.2017.00980. 2017.

Yeh, P.J., and Famiglietti, J.S.: Regional Groundwater Evapotranspiration in Illinois. J. Hydrometeorol., 10:464-478. https:// doi.org/ 10.1175/2008JHM1018.1. 2009.

Zammouri, M.: Case Study of Water Table Evaporation at Ichkeul Marshes (Tunisia). J. Irrig. Drain. Eng., 127:265-271. https:// doi.org/10.1061/(ASCE)0733-9437(2001)127：5(265). 2001.